

Nanostructures on glass surfaces fabricated using HF gas-etching for reducing adhesion forces of dust particles

Ryudai Nitano¹, Shuntaro Yamato², Nobuya Mineyuki^{3,4}, Kohei Yasuda³, and Masato Adach^{1,*}

¹Department of Mechanical Engineering and Science, Kyoto University, Kyoto 615-8540, Japan

²Department of Mechanical Systems Engineering, Tokyo University of Agriculture and Technology, Tokyo 184-8588, Japan

³Innovative Technology Laboratories, AGC Inc., Yokohama 230-0045, Japan

⁴Graduate School of Advanced Science and Engineering, Hiroshima University, Hiroshima 739-8530, Japan

Abstract. The formation of nanostructures on glass surfaces is an effective dust mitigation strategy for optical devices used in both terrestrial and space environments. This approach requires reducing dust particle adhesion while maintaining the excellent optical properties of the glass. In this study, nanostructures with varying surface roughness were successfully fabricated on glass substrates through hydrogen fluoride (HF) gas etching. Additionally, the adhesion forces between the glass surfaces and particles, as well as the transmittance of the glass, were experimentally evaluated. The results revealed a trade-off between reducing particle adhesion and increasing visible light transmittance. Furthermore, it was successfully demonstrated that both requirements could be reconciled by optimizing the processing temperature during HF gas etching.

1 Introduction

Particulate materials are widely used across various industrial fields and naturally exist in both terrestrial and space environments. During the handling of particulate materials, dust contamination on equipment surfaces presents significant challenges, degrading functionality and causing malfunctions. For instance, frequent sandstorms in desert regions lift large amounts of dust, which then accumulate on critical infrastructure such as solar panels, significantly reducing power generation efficiency [1]. Similar issues arise in space exploration missions, where regolith particles covering the surfaces of the Moon and Mars are easily lifted due to lower gravity and readily adhere to optical lenses, thermal control materials, and the spacesuit visors, posing substantial risks to both manned and unmanned missions [2].

In such dusty environments, effective dust-proof and dust-removal technologies are indispensable, particularly for glass materials that require high optical and thermal properties, which are degraded by deposited dust particles. One key strategy to address this issue is reducing the adhesion forces between small particles and the glass surface [3]. A promising approach to achieve this involves fabricating nanostructures on glass surfaces, which not only provide dust-proof properties but also enhance the effectiveness of other dust removal techniques [4]. These nanostructures alter the effective distance between materials at the contact interface, thereby reducing van der Waals forces—the dominant forces for particles with smaller diameters [5]. The effects of surface roughness on reducing particle adhesion have been widely investigated for metallic

materials, whose surface roughness can be relatively easily modified, leading to applications across various industries [6, 7]. However, the formation of uniform surface nanostructures on glass and their impact on dust particle adhesion have not been sufficiently studied. Furthermore, the secondary effects of surface nanostructures on key practical functionalities, such as the optical properties required for glass materials, remain unclear.

In this study, we fabricated glass substrates using a hydrogen fluoride (HF) gas etching method, which enables both high production efficiency and high precision processing. This technique allowed for the preparation of substrates with varying surface roughness. Additionally, the adhesion forces between the glass surfaces and particles were experimentally measured using atomic force microscopy, and we evaluated the influence of the fabricated nanostructures on the optical properties of the glass substrates.

2 Experimental method

2.1 Formation of nanostructures on glass

Soda-lime glass was used as the substrate, with dimensions of 10 mm × 10 mm and a thickness of 1 mm. The substrates were treated with HF gas under atmospheric pressure for 4 seconds, followed by cleaning with 10 % hydrochloric acid [8]. Surface roughness was controlled by varying the treatment temperature to 400, 500, 600, and 650 °C. Figure 1 shows cross-sectional images of untreated and treated substrates observed using scanning electron microscopy

* Corresponding author: masato@me.kyoto-u.ac.jp

(SEM: Hitachi High-Tech, SU8030) [9]. The surface morphology and roughness were examined using atomic force microscopy (AFM: Shimadzu, SPM-9700HT) over a $5\ \mu\text{m} \times 5\ \mu\text{m}$ scanning area at three different locations on each sample. Figure 2 shows the surface profiles and root mean square (RMS) roughness of the substrates. As shown in Figs. 1 and 2, HF gas etching enabled relatively uniform processing across the entire substrate, and increasing treatment temperature resulted in larger surface nanostructures. At $400\ \text{}^\circ\text{C}$, concave structures formed on the substrate, while at $650\ \text{}^\circ\text{C}$, large convex structures appeared, leading to a sharp increase in RMS roughness.

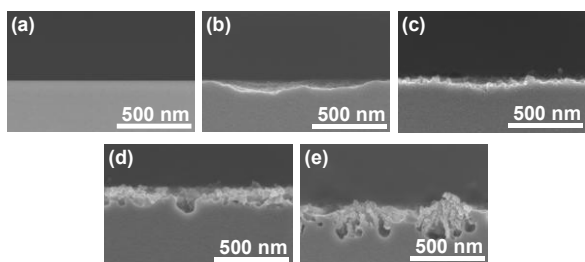


Fig. 1. SEM images of the cross sections of (a) the untreated substrate and (b–e) the HF-etched substrates treated at different temperatures: (b) $400\ \text{}^\circ\text{C}$, (c) $500\ \text{}^\circ\text{C}$, (d) $600\ \text{}^\circ\text{C}$, and (e) $650\ \text{}^\circ\text{C}$ [9].

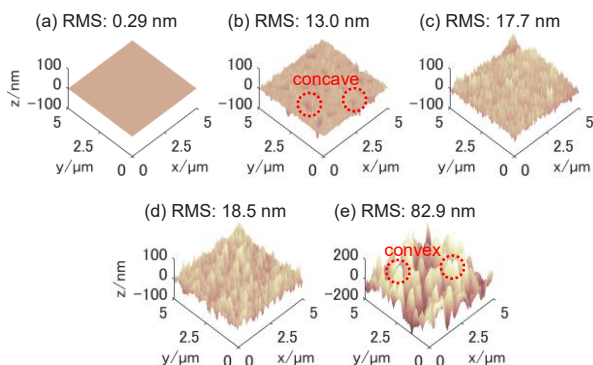


Fig. 2. Surface profiles and RMS roughness of (a) the untreated substrate and (b–e) the HF-etched substrates treated at (b) $400\ \text{}^\circ\text{C}$, (c) $500\ \text{}^\circ\text{C}$, (d) $600\ \text{}^\circ\text{C}$, and (e) $650\ \text{}^\circ\text{C}$.

2.2 Measurement

Figure 3 illustrates a schematic of the adhesion force measurement between a particle and a substrate using an AFM. The AFM probes were fabricated by attaching a spherical glass particle (AS ONE, soda-lime glass) or a lunar regolith simulant particle with an irregular shape (Shimizu Corporation, FJS-1) to the tip of the AFM cantilever using epoxy resin. The regolith simulant was manufactured resembling actual lunar dust particles with complex geometries. A single particle was used for all measurements under each probe type condition, without replacement. Figure 4 shows the probe particles. The adhesion force measurement was conducted by detecting the deflection of the cantilever during the particle-substrate contact process, providing a force–displacement curve. The adhesion force was calculated

from the force curve as the attractive force acting on the cantilever when the probe detached from the substrate.

This adhesion force measurement was conducted over a scanning area of $500\ \text{nm} \times 500\ \text{nm}$ on the substrates, providing a distribution of the force. Furthermore, the approach and detachment processes enabled the simultaneous acquisition of the surface profile, as shown in Fig. 5. Since the spatial distribution of surface roughness can also be derived from the surface profile, the distributions of adhesion force and surface roughness can be compared. We defined two types of RMS roughness: conventional RMS roughness shown in Fig. 2, which represents the standard deviation of the height distribution for the entire scanning area of the substrate; and localized RMS roughness, which is defined as the RMS roughness distribution within smaller divided areas of the substrate. The size of these divisions was determined based on the Hertzian contact theory between a spherical particle and a smooth substrate [6, 9]. Considering the particle size and contact pressure, the contact area was estimated to be approximately $30\ \text{nm} \times 30\ \text{nm}$. The resolution of the data points during the AFM process was 128×128 within a scanning area of $500\ \text{nm} \times 500\ \text{nm}$. The area was divided into 31 nm sections, resulting in 16×16 data points for both localized RMS roughness and average adhesion force.

The adhesion forces and surface profiles were measured for various combinations of probe particles and substrates with different surface roughness levels. Each scan was conducted three times at different locations on the substrate, and the relationship between force and roughness distributions was quantified. All measurements were performed at room temperature and atmospheric pressure, with relative humidity maintained at 40–50 % using a humidifier (KITZ Microfilter, AHCU-2).

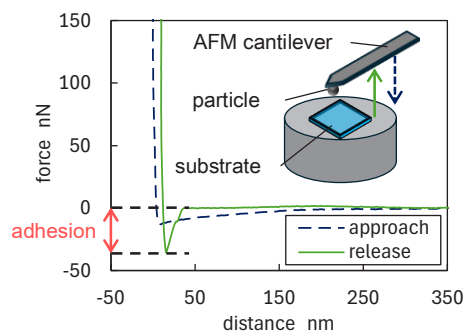


Fig. 3. Adhesion force measurement from the force–displacement curve using AFM.

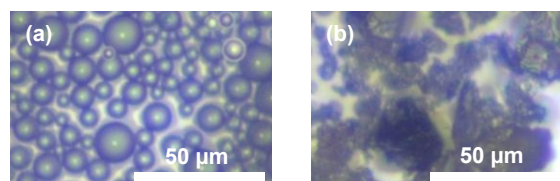


Fig. 4. Optical microscope images of (a) the spherical glass particles and (b) the regolith simulant.

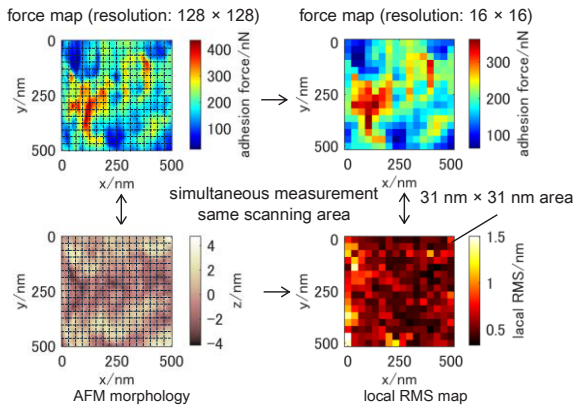


Fig. 5. Simultaneous measurement of the distributions of the adhesion force and localized RMS roughness.

Additionally, the transmittance of the substrates was measured in the visible wavelength range (380–780 nm) using a spectrophotometer (JASCO, V-670).

3 Results and discussion

Figure 6 shows the distribution of adhesion forces with respect to the localized RMS roughness between the 3 μm diameter spherical glass particle and both untreated and HF gas-etched substrates. The adhesion force was significantly reduced by HF gas etching treatment. The treated substrate caused a reduction in the proximity contact area with the particle, decreasing the effective energy of van der Waals interactions at the surface. In addition, the untreated substrate exhibited a narrow distribution of adhesion forces, whereas the HF gas-etched substrates showed wider distributions. Moreover, the distribution broadened as the HF gas etching treatment temperature increased. As shown in Fig. 1, the surface nanostructures became larger and more uneven with increasing treatment temperature. This unevenness of the surface roughness resulted in a broader distribution of adhesion forces.

Additionally, Fig. 6 presents the theoretical van der Waals forces F_{vdW} calculated using Eq. (1), known as the modified Rumpf model [5]:

$$F_{vdW} = \frac{AR}{6H_0^2} \left[\frac{1}{1 + \frac{R}{1.48rms}} + \frac{1}{\left(1 + \frac{1.48rms}{H_0}\right)^2} \right] \quad (1)$$

where, A is the Hamaker constant (10^{-19} J), R is the particle radius (1.5 μm), H_0 is the distance of closest approach between surfaces (approximately 0.3 nm), and rms is the RMS roughness of the surface contacting with the particle. As shown in Fig. 6, the experimentally measured values agreed well with the theoretical predictions, although some discrepancies remained. The measured adhesion forces were higher than those predicted by the model, likely due to additional contributions from the electrostatic and capillary forces present in the experimental measurements. However, van der Waals forces were the primary contributors to the experimentally measured adhesion force, which was

mitigated by the presence of nanostructures. Moreover, the adhesion force decreased as the localized surface roughness increased up to several nanometers.

Figure 7 shows the adhesion forces of the spherical glass particle and the regolith simulant, both with a diameter of approximately 10 μm, on the substrates. The adhesion force of irregularly shaped dust particle also decreased as the RMS roughness of the substrate increased. For the untreated substrate, which exhibited the lowest RMS roughness, the adhesion force of the regolith simulant was lower than that of the spherical glass particles. Conversely, on the HF gas-etched substrates, the adhesion force of the regolith simulant exceeded that of the spherical glass particles. This is because the surface roughness of the particles themselves also influences adhesion. Figure 8 shows the surface profiles of the particles measured using AFM. The regolith simulant exhibited a higher RMS roughness than the spherical glass particles, reducing the contact area between the regolith particle and a flat surface. In contrast, as illustrated in Fig. 9, the irregular and multifaceted particle increased the number of contact points with the HF gas-etched substrates compared with the spherical particle. As a result, the adhesion-reducing effect of surface roughness was less pronounced for the regolith simulant than for the spherical particle.

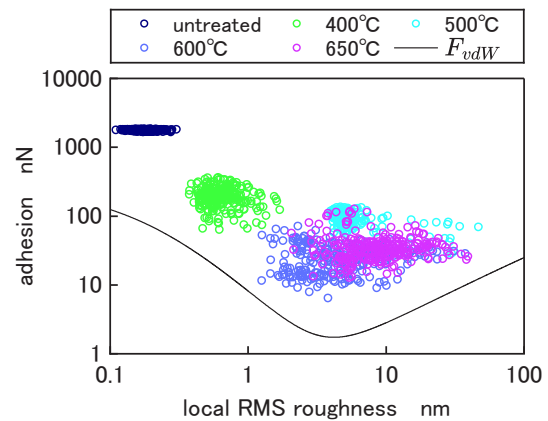


Fig. 6. Adhesion force distribution with respect to localized RMS roughness for the spherical glass particle on untreated and treated glass substrates.

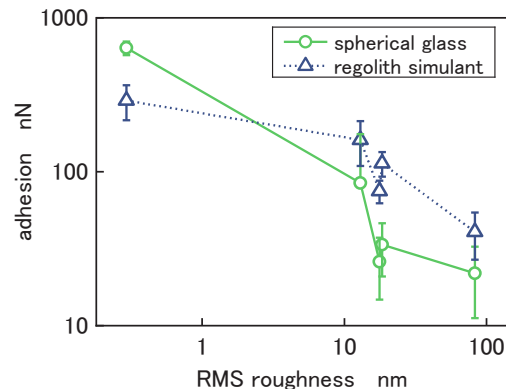


Fig. 7. Adhesion forces of the spherical glass particle and the regolith simulant on substrates with different RMS roughness.

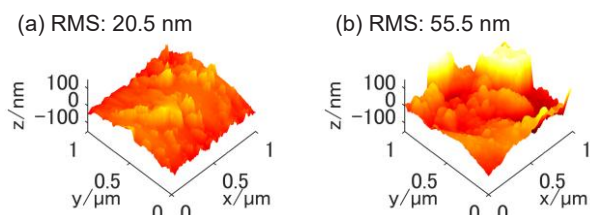


Fig. 8. Surface profiles and the RMS roughness of (a) the spherical glass particle and (b) the regolith simulant.

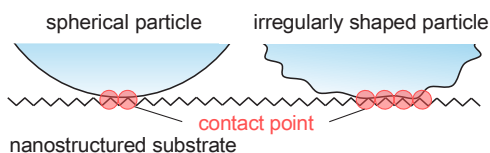


Fig. 9. Schematics of the contact models between a nanostructured substrate and a spherical particle, as well as an irregularly shaped particle with roughness.

In addition to particle adhesion characteristics, the effects of surface nanostructures on optical properties were investigated. Figure 10 shows the relationship between the average transmittance [9] and the mean adhesion force of spherical glass particles with a diameter of 10 μm . An increase in transmittance was observed up to 600°C, attributed to an antireflection effect, where surface nanostructures create a gradual refractive index gradient in the visible wavelength region [9]. In contrast, the decrease in transmittance from 600°C to 650°C was due to increased light scattering caused by large convex structures formed on the surface treated at 650 °C, as shown in Fig. 2. These results indicate that surface nanostructures affect both adhesion and light transmittance, and the optimal HF gas etching temperature enables the reduction of adhesion force while simultaneously enhancing optical properties.

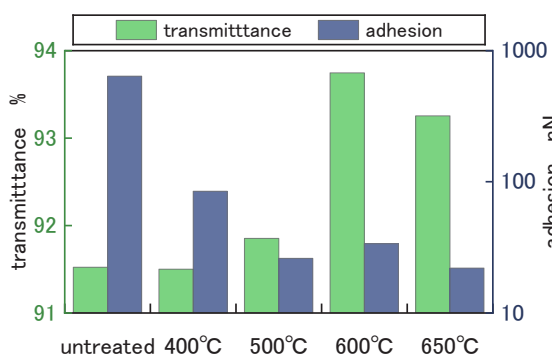


Fig. 10. Relationship between the averaged transmittance in the visible wavelength range and the mean adhesion force between the spherical glass particle and the substrates.

4 Conclusions

In this study, the effects of surface nanostructures formed on glass by HF gas etching were investigated with respect to reducing the adhesion force between the glass surface and particles. In addition, the influence of

these nanostructures on the optical transmittance of the processed glass was experimentally evaluated. The HF gas treatment significantly reduced the adhesion force. Moreover, the gas etching process, which was optimized at specific temperatures, simultaneously enhanced the light transmittance of the glass within the visible spectrum. Thus, HF gas-etched glass may serve as an effective dust-resistant material for use in a wide range of optical systems.

References

1. A. Sayyah, M. N. Horenstein, and M. K. Mazumder, Energy yield loss caused by dust deposition on photovoltaic panels. *Sol. Energy* **107**, 576 (2014).
<https://doi.org/10.1016/j.solener.2014.05.030>
2. J. R. Gaier, The Effects of Lunar Dust on EVA Systems During the Apollo Missions. NASA Glenn Research Center, (2007)
<https://ntrs.nasa.gov/citations/20070021819>
3. R. J. Isaifan, D. Johnson, L. Ackermann, B. Figgis, and M. Ayoub, Evaluation of the adhesion forces between dust particles and photovoltaic module surfaces. *Sol. Energy Mater. Sol. Cells* **191**, 413 (2019).
<https://doi.org/10.1016/j.solmat.2018.11.031>
4. P. Zanon, M. Dunn, and G. Brooks, Current Lunar dust mitigation techniques and future directions. *Acta Astronaut.* **213**, 627 (2023).
<https://doi.org/10.1016/j.actaastro.2023.09.031>
5. Y. I. Rabinovich, J. J. Adler, A. Ata, R. K. Singh, and B. M. Moudgil, Adhesion between nanoscale rough surfaces: I. Role of asperity geometry. *J. Colloid Interface Sci.* **232**, 10 (2000).
<https://doi.org/10.1006/jcis.2000.7167>
6. T. Miwa, G. Miya, and S. Kanno, Effect of surface roughness on small particle adhesion forces evaluated by atomic force microscopy. *Jpn. J. Appl. Phys.* **59**, 076504 (2020).
<https://doi.org/10.35848/1347-4065/ab9e48>
7. X. Wang, W. Wang, H. Shao, S. Chao, H. Zhang, C. Tang, X. Li, Y. Zhu, J. Zhang, X. Zhang, and Y. Lu, Lunar Dust-Mitigation Behavior of Aluminum Surfaces with Multiscale Roughness Prepared by a Composite Etching Method. *ACS Appl. Mater. Interfaces* **14**, 34020 (2022).
<https://doi.org/10.1021/acsami.2c07237>
8. K. Yasuda, Y. Hayashi, and T. Homma, Fabrication of Superhydrophobic Nanostructures on Glass Surfaces Using Hydrogen Fluoride Gas. *ACS Omega* **9**, 12204 (2024).
<https://doi.org/10.1021/acsomega.4c00170>
9. H.-J. Butt, B. Cappella, and M. Kappell, Force measurements with the atomic force microscope: Technique, interpretation and applications. *Surf. Sci. Rep.* **59**, 1 (2005).
<https://doi.org/10.1016/j.surfrep.2005.08.003>